

Formation, photodissociation and structure of chromium/phosphorus binary cluster ions

Chunying Han, Xiang Zhao, Xia Zhang, Zhen Gao* and Qihe Zhu

State Key Laboratory of Molecular Reaction Dynamics, Center of Molecular Science, Institute of Chemistry, Chinese Academy of Sciences, Beijing 100080, People's Republic of China

Chromium/phosphorus binary cluster ions, $[\text{Cr}_n\text{P}_m]^{\pm}$, produced by laser (532nm) ablation on a tablet of well-mixed chromium and red phosphorus powder, were studied with a home-built tandem time-of-flight (TOF) mass spectrometer. The clusters thus formed are mostly rich in phosphorus. There is an odd-even oscillation in the intensity of the $[\text{CrP}_m]^+$ series, i.e. the mass peaks of even m are higher than those of odd m . The peaks of $[\text{CrP}_4]^+$ and $[\text{CrP}_8]^+$ are especially prominent, which may be ascribed to the specific stability of P_4 sub-structures. There are also some intense peaks in the spectrum assigned to $[\text{Cr}_3\text{P}_8]^+$, $[\text{Cr}_4\text{P}_9]^+$, $[\text{Cr}_5\text{P}_{11}]^+$, $[\text{Cr}_6\text{P}_{12}]^+$, $[\text{Cr}_8\text{P}_{14}]^+$ clusters, etc., which have stable compositions. The stability of these species is consistent with a simple qualitative electronic structure model, in which the valence electrons of P are filled into the d orbitals of Cr. The photodissociation of some cluster ions was also studied. DFT calculations were performed on three small cluster ions to provide some insight into their structures. Copyright © 2000 John Wiley & Sons, Ltd.

Received 25 April 2000; Revised 19 May 2000; Accepted 23 May 2000

In the past decade, binary clusters composed of transition metal and non-metal elements have attracted much interest because of their remarkable electronic and structural characteristics, and their applications in many fields.^{1–4} However, in the previous work on clusters of this kind, the non-metal elements have mainly been C,^{5,6} O,^{7,9} S^{9–12} and Se.^{13,14} In this paper we report the study of clusters composed of transition metals and phosphorus. An earlier paper¹⁵ reported Co/P and Ni/P binary cluster ions produced by laser (1064 nm) ablation on mixtures of the metals and red phosphorus, and analyzed using Fourier transform ion cyclotron resonance mass spectrometry (FTICRMS). Because the high vapor pressure of red phosphorus is not compatible with the low-pressure detection requirements of FTICRMS, the ions studied in these experiments contained only a few phosphorus atoms and the clusters contained only one metal atom.

Phosphides of transition metals comprise a very large class of compounds.¹⁶ Many transition metals can form more than one type of phosphide, and most of them are polymorphic. As regards bonding in phosphides, they present a wide variety, i.e. ionic and covalent to essentially metallic. The phosphides were found to have chain, ring, cage or layer structures, and to have many important applications in many fields.¹⁷ Iron phosphide is used to prepare high-strength steel, Ir₂P has been used to make the tips of pens because of its chemical stability and hardness, copper phosphide usually acts as an oxygenating reagent, etc. In addition, P is the neighbouring element of S in the Periodic Table, and the two elements, P and S, are somewhat similar in character,¹⁷ e.g. their elemental forms

are polyatomic species, more than one allotrope exists, both P and S have empty d orbitals to use in bonding, etc.

In this paper, we report our experimental investigation of chromium/phosphorus cluster ions using a home-built tandem time-of-flight mass spectrometer (Tandem TOFMS). Unlike FTICRMS, the Tandem TOFMS is not affected by the high vapor pressure of red phosphorus, so we were able to investigate more samples of different compositions including those richer in phosphorus, such as Cr/P = 1:6.

EXPERIMENTAL

The samples were prepared with chromium (purity >98%) and purified red phosphorus powder, mixed in different atomic ratios and pressed into tablets.

Experiments were performed on the Tandem TOFMS; the details have been published elsewhere.^{10,18} In brief, the solid sample was held in a vacuum chamber at 10^{-6} Torr and the second harmonic of a Nd:YAG laser (532 nm, ~10 mJ/pulse, ~8 ns/pulse, 10 Hz) was focused on the surface of the sample to a spot of 0.5 mm diameter. The cluster ions produced by laser ablation were extracted, accelerated by a pulsed electric field of 0.1 kV/30 mm and 1.1 kV/10 mm, respectively, and then drifted along a 3.5 m-long field-free flight tube. The cluster ions with different mass were detected by the dual microchannel plates. The mass resolution of the first stage of the Tandem TOFMS is about 300. Cluster cations with a specific mass number can be selected by the mass gate, at the end of the first stage flight tube, which is operated by a pulsed voltage. The selected cations, after deceleration, were photodissociated with a UV excimer laser (Lambda Physik LPX300, KrF, 248 nm wavelength, 10 Hz, 200–400 mJ/pulse, ~20 ns/pulse). The daughter ions and the remaining parent ions were all reaccelerated and analyzed by the second stage of the Tandem TOFMS which is perpendicular to the first

*Correspondence to: Zhen Gao, State Key Laboratory of Molecular Reaction Dynamics, Center of Molecular Science, Institute of Chemistry, Chinese Academy of Sciences, Beijing 100080, People's Republic of China.

Contract/grant sponsor: The National Science Foundation of China.

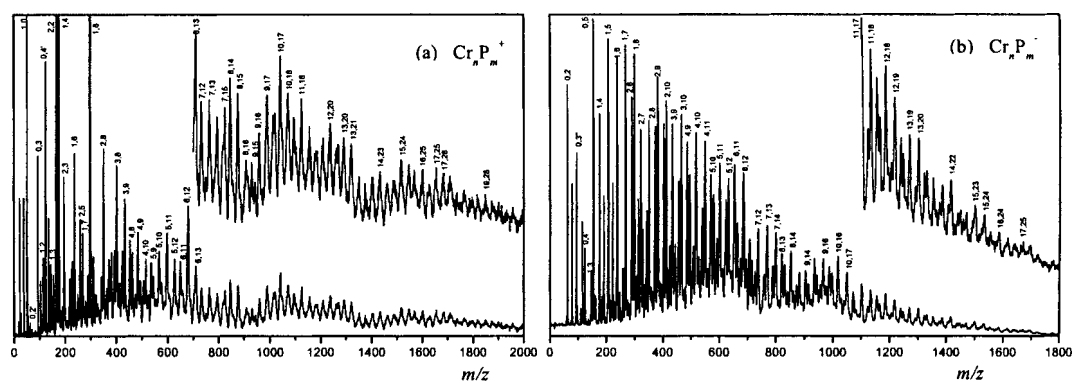


Figure 1. TOF mass spectra of Cr/P cluster ions produced by laser ablation on a mixed sample with Cr/P = 1:1. (a) Cations $[Cr_nP_m]^+$ and (b) anions $[Cr_nP_m]^-$.

stage and has a flight tube 1.5 m long. The detector of the second stage of the spectrometer is another dual micro-channel plate arrangement. The signals from the two stages were recorded using a transient recorder (10 MHz), pre-amplified and stored in a personal computer.

RESULTS

Formation of Cr/P binary cluster ions

In order to obtain the distribution characteristics of Cr/P cluster ions, several samples at atomic ratios Cr/P = 8:1, 3:1, 1:1 and 1:6 were investigated. Typical TOF mass spectra of Cr/P cluster cations and anions, produced by laser ablation on samples of atomic ratio Cr/P = 1:1 and Cr/P = 1:6, are shown in Figs 1 and 2, respectively. The mass peaks are labeled with (n,m) corresponding to the numbers of Cr atoms (n) and of P atoms (m) in the cluster cations and anions, respectively.

By comparing the mass spectra from the samples at different atomic ratios, we find the following characteristics of the cluster distribution. (1) The binary cluster cations and anions, $[Cr_nP_m]^\pm$, were mainly rich in phosphorus ($m > n$), especially for the cluster anions, which were all rich in phosphorus. (2) The cluster cations with $m < n$ were found only for $n \leq 3$, and their intensities are all relatively weak. (3) With the increase of n in $[Cr_nP_m]^\pm$, $(m-n)$ becomes larger, even in the case of samples with low phosphorus content, such as Cr/P = 8:1. In addition, the cluster ions, $[H_xP_m]^+$ ($m = 2-5$) and $[H_xP_m]^-$ ($m = 2-9$) appeared also in

the mass spectra, but their intensities were much weaker, except for $[H_2P_3]^-$ and $[P_5]^-$. It was noticed that, for even values of m in $[H_xP_m]^\pm$, the number of hydrogen atoms, x , is usually odd (1 or 3), while for odd m , x is even (0 or 2, labelled as 0,2', 0,3'' and 0,4''', etc. in the spectra).

The experiments also show that the atomic ratio Cr/P in the sample does not affect the cluster ion distribution much, but the larger clusters can be formed more easily when the phosphorus content is higher in the sample.

$[CrP_m]^\pm$ cluster ions exhibit a prominent intensity in the mass spectra, with an odd-even oscillation, in which the peaks with even m are much higher than those with odd m . In particular $[CrP_4]^+$ and $[CrP_8]^+$ are the most intense peaks, while $[CrP]^+$ and $[CrP_5]^+$ are almost not seen in the spectra.

It is important to note that $[Cr_3P_8]^+$, $[Cr_4P_9]^+$, $[Cr_5P_{11}]^+$, $[Cr_6P_{12}]^+$, $[Cr_8P_{14}]^+$, $[Cr_{10}P_{17}]^+$, $[Cr_{15}P_{24}]^+$, etc., are always present at high intensity in the mass spectra, while for cluster anions, there are no apparent local intensity maxima among the mass peaks in the spectra.

UV photodissociation of Cr/P binary cluster cations

The photodissociation of some $[Cr_nP_m]^+$ cluster cations was performed. Cluster cations of a specific mass number were selected by the mass gate in the Tandem TOFMS and photodissociated by a 248 nm laser. The results of photodissociation are summarized in Table 1. The photodissociation efficiency, R_i , of each channel can be calculated by the formula $R_i = I_i / \sum_j I_j$, where I_i is the

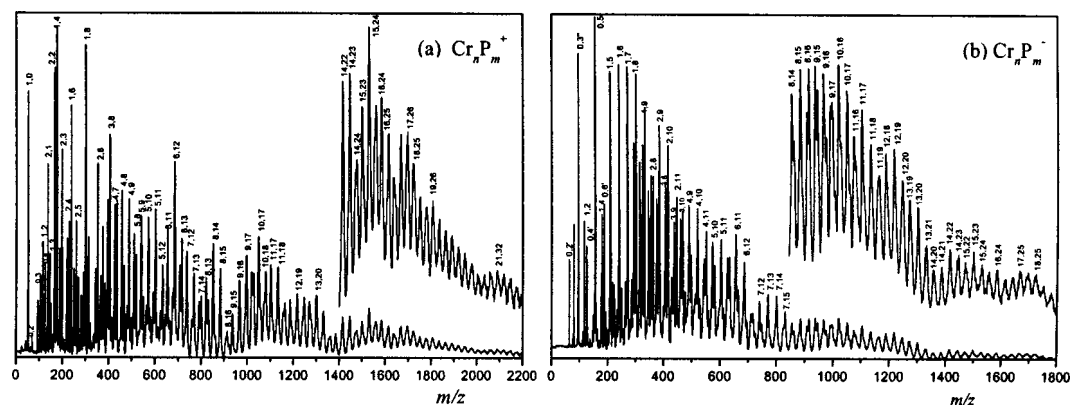


Figure 2. TOF mass spectra of Cr/P cluster ions produced by laser ablation on a mixed sample with Cr/P = 1:6. (a) Cations $[Cr_nP_m]^+$ and (b) anions $[Cr_nP_m]^-$.

Table 1. Photodissociation channels and efficiency of Cr/P binary cluster cations

| Parent ions | Channel | R _i (%) | ΣR _i (%) | Parent ions | Channel | R _i (%) | ΣR _i (%) |
|--|--|--------------------|---------------------|--|--|--------------------|---------------------|
| [CrP ₄] ⁺ | [CrP ₂] ⁺ + (P ₂) | 4.76 | 9.56 | [Cr ₃ P ₈] ⁺ | [Cr ₃ P ₆] ⁺ + (P ₂) | 3.00 | 48.50 |
| | [Cr] ⁺ + (P ₄) | 4.80 | | | [Cr ₃ P ₄] ⁺ + (P ₄) | 26.89 | |
| [CrP ₆] ⁺ | [CrP ₄] ⁺ + (P ₂) | 2.13 | 14.32 | [Cr ₄ P ₈] ⁺ | [Cr ₃ P ₂] ⁺ + (P ₆) | 16.74 | 43.09 |
| | [CrP ₂] ⁺ + (P ₄) | 12.19 | | | [Cr ₂ P ₂] ⁺ + (CrP ₆) | 1.87 | |
| [CrP ₈] ⁺ | [CrP ₄] ⁺ + (P ₄) | 8.03 | 8.03 | [Cr ₄ P ₆] ⁺ + (P ₂) | 15.12 | 19.53 | 47.17 |
| [Cr ₂ P ₂] ⁺ | [Cr ₂ P] ⁺ + (P) | 0.77 | 9.76 | [Cr ₄ P ₄] ⁺ + (P ₄) | 19.53 | | |
| | [Cr ₂] ⁺ + (P ₂) | 3.24 | | [Cr ₄ P ₂] ⁺ + (P ₆) | 6.86 | | |
| [Cr ₂ P ₃] ⁺ | [Cr] ⁺ + (CrP ₂) | 5.75 | 10.43 | [Cr ₅ P ₁₁] ⁺ | [Cr ₃ P ₂] ⁺ + (CrP ₆) | 1.58 | 47.17 |
| | [Cr ₂ P ₂] ⁺ + (P) | 1.50 | | [Cr ₅ P ₉] ⁺ + (P ₂) | 11.91 | | |
| | [Cr ₂ P] ⁺ + (P ₂) | 7.33 | | [Cr ₅ P ₇] ⁺ + (P ₄) | 22.20 | | |
| | [Cr ₂] ⁺ + (P ₃) | 0.61 | | [Cr ₅ P ₅] ⁺ + (P ₆) | 13.06 | | |
| [Cr ₂ P ₅] ⁺ | [Cr] ⁺ + (CrP ₃) | 0.99 | 6.57 | [Cr ₆ P ₁₂] ⁺ | [Cr ₆ P ₁₀] ⁺ + (P ₂) | 16.89 | 60.21 |
| | [Cr ₂ P ₃] ⁺ + (P ₂) | 4.46 | | [Cr ₅ P ₁₀] ⁺ + (CrP ₂) | 14.80 | | |
| [Cr ₂ P ₈] ⁺ | [Cr ₂ P] ⁺ + (P ₄) | 2.11 | 24.20 | [Cr ₅ P ₈] ⁺ + (CrP ₄) | 14.47 | 4.45 | 4.32 |
| | [Cr ₂ P ₄] ⁺ + (P ₄) | 6.68 | | [Cr ₅ P ₆] ⁺ + (CrP ₆) | 5.28 | | |
| | [Cr ₂ P ₂] ⁺ + (P ₆) | 17.52 | | [Cr ₄ P ₆] ⁺ + (Cr ₂ P ₆) | 4.45 | | |
| | | | | [Cr ₄ P ₄] ⁺ + (Cr ₂ P ₈) | 4.32 | | |

intensity of daughter ion *i* and $\sum I_j$ is the total intensity of daughter ions and the surviving parent ion.

From Table 1, it can be seen that for the parent [Cr_{*n*}P_{*m*}]⁺ (*m* > *n*) clusters, the main photodissociation channel is loss of P₂ or P₄, while the channel with loss of P or P₃ did not appear. After successive loss of P₂ or P₄ until the numbers of Cr and P atoms are close, the loss of Cr atoms occurs. As shown in Fig. 3, a typical mass spectrum from the photodissociation of [Cr₃P₈]⁺, four photodissociation channels exist giving [Cr₃P₆]⁺, [Cr₃P₄]⁺, [Cr₃P₂]⁺ and [Cr₂P₂]⁺ daughter ions, among which [Cr₃P₄]⁺ is the most abundant daughter ion and, after loss of P₂ plus P₄, expulsion of Cr occurred to form [Cr₂P₂]⁺. However, for [Cr₆P₁₂]⁺ photodissociation, the loss of P₂ is the main channel (shown in Fig. 4), and then the expulsion of Cr began to occur. The smallest daughter ion in this case was [Cr₄P₄]⁺, with a total loss of Cr₂P₈.

Theoretical calculations

Three small cluster ions, [CrP₄]⁺, [CrP₈]⁺ and [Cr₂P₂]⁺, were selected for quantum-chemical calculations. 3-21G* was used as the basis set, and the B3LYP method was chosen for calculation. The method has already been tested and shown to be suitable for transition metal/non-metal binary cluster ions.¹⁴

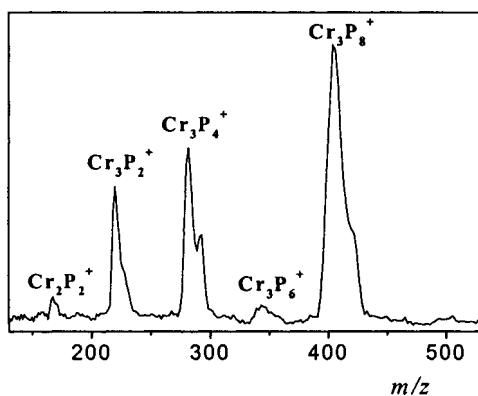


Figure 3. TOF mass spectrum of photodissociation products of [Cr₃P₈]⁺.

For [CrP₄]⁺, ten structural models were assumed. The optimized configurations and the calculated energies are shown in Fig. 5. For [CrP₈]⁺ and [Cr₂P₂]⁺, we calculated three and four configurations, respectively, and these results are given in Figs 6 and 7.

DISCUSSION

Formation and photodissociation of Cr/P cluster ions

The Cr/P binary cluster ions are almost all rich in phosphorus, implying that P-P bonds may exist in the clusters. In the mass spectra, phosphorus cluster ions [P_{*m*}][±] were also produced, but their size *m* is only up to 5 for cations and 9 for anions, and their intensities are relatively weak. In comparison, with laser ablation on a pure phosphorus sample, cluster ions [P_{*m*}][±] with *m* up to 23 can be produced. This result indicates that the clustering between Cr and P is stronger than that between P and P.

The experiments indicate that a higher phosphorus content in the sample is helpful to the formation of large clusters. The reason might be due to the volatility of red phosphorus. During laser ablation, dense phosphorus vapor could produce a strong cooling effect on the expansion of the vapor into the vacuum.¹⁹

The odd-even oscillation in intensity of the [CrP_{*m*}]⁺ series, and the high stability of [CrP₄]⁺ and [CrP₈]⁺, may be

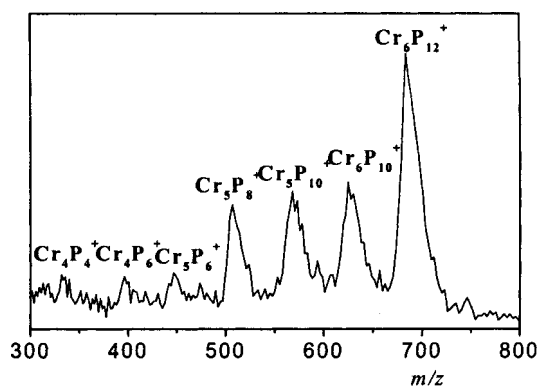


Figure 4. TOF mass spectrum of photodissociation products of [Cr₆P₁₂]⁺.

Table 2. Number of d orbitals of Cr atoms and number of valence electrons of $[\text{Cr}_n\text{P}_m]^+$

| $[\text{Cr}_n\text{P}_m]^+$ | Number of d orbitals of Cr atoms | Number of valence electrons |
|-----------------------------------|----------------------------------|----------------------------------|
| $[\text{Cr}_3\text{P}_8]^+$ | 15 | $29 + 2(\leftarrow \text{P}_4)$ |
| $[\text{Cr}_4\text{P}_9]^+$ | 20 | $38 + 2(\leftarrow \text{P}_4)$ |
| $[\text{Cr}_5\text{P}_{11}]^+$ | 25 | $50 + 2(\leftarrow \text{P}_4)$ |
| $[\text{Cr}_6\text{P}_{12}]^+$ | 30 | $59 + 2(\leftarrow \text{P}_4)$ |
| $[\text{Cr}_8\text{P}_{14}]^+$ | 40 | $77 + 2(\leftarrow \text{P}_4)$ |
| $[\text{Cr}_{10}\text{P}_{17}]^+$ | 50 | $98 + 2(\leftarrow \text{P}_4)$ |
| $[\text{Cr}_{13}\text{P}_{20}]^+$ | 65 | $125 + 2(\leftarrow \text{P}_4)$ |
| $[\text{Cr}_{14}\text{P}_{23}]^+$ | 70 | $140 + 2(\leftarrow \text{P}_4)$ |
| $[\text{Cr}_{15}\text{P}_{24}]^+$ | 75 | $149 + 2(\leftarrow \text{P}_4)$ |

Note: '+2' in the third column of this table means the two electrons from P_4 coordination unit were offered to the cluster.

ascribed to the specific stability of the P_4 structure.¹⁷ P_4 is the structural unit of white phosphorus and is the main component of phosphorus vapor, with a stable tetrahedron structure. As the temperature increases, the chemical equilibrium $\text{P}_4(\text{g}) \rightleftharpoons 2\text{P}_2(\text{g})$ is displaced to the right. Thus, after laser ablation, during the plasma expansion and cooling, P_2 or P_4 dominates the vapor. This could be the reason why the mass peaks of $[\text{CrP}_m]^+$ with even m are more intense. The photodissociation experiments show that the main channel of $[\text{CrP}_m]^+$ photodissociation is the loss of P_2 or P_4 , therefore we can conclude that P atoms mainly exist as P_2 or P_4 in $[\text{CrP}_m]^+$ clusters.

In the study of clusters, one is usually more interested in higher mass peaks. In our experiments, the higher mass peaks $[\text{Cr}_3\text{P}_8]^+$, $[\text{Cr}_4\text{P}_9]^+$, $[\text{Cr}_5\text{P}_{11}]^+$, $[\text{Cr}_6\text{P}_{12}]^+$, $[\text{Cr}_8\text{P}_{14}]^+$, $[\text{Cr}_{10}\text{P}_{17}]^+$, $[\text{Cr}_{15}\text{P}_{24}]^+$, etc. are prominent in the mass

spectra. It is interesting that, if a P_4 unit is removed from any one of these clusters, the number of valence electrons in these clusters is nearly twice the number of d orbitals of the Cr atoms. The details are shown in Table 2, supposing that three valence electrons of each P and the 4s electron of each Cr atom all move into 3d orbitals during clustering.

In this model, the P_4 unit in these clusters behaves as a coordinating unit. This can also rationalize the photodissociation experiments with loss of P_4 . For example, the main photodissociation channel of $[\text{Cr}_3\text{P}_8]^+$ was loss of P_4 (shown in Fig. 3), and $[\text{Cr}_5\text{P}_7]^+$ was also the main photodissociation product of $[\text{Cr}_5\text{P}_{11}]^+$, showing that P_4 has weak interaction with the other part of the clusters and is easily stripped off. The exception to this rule is the cluster $[\text{Cr}_6\text{P}_{12}]^+$, from which P_2 was stripped as the main channel of photodissociation, but this might be due to the special geometry of $[\text{Cr}_6\text{P}_{12}]^+$.

For Cr/P crystalline compounds, there are two types of compositions: Cr_3P and CrP^{17} , which are apparently different from Cr/P clusters. This means that Cr/P crystals and Cr/P cluster ions have different structures and bonding modes.

Structure and stability of Cr/P binary cluster ions

Structural models for the clusters $[\text{CrP}_4]^+$, $[\text{CrP}_8]^+$ and $[\text{Cr}_2\text{P}_2]^+$ were assumed and their energies computed as described above.

Ten structural models of $[\text{CrP}_4]^+$ were proposed, and Fig. 5 shows the results of the energy calculations. We can observe that the structures (h) (i) (j), incorporating a P_4 tetrahedron, are more stable than the other linear or planar structures, and the most stable structure (i) has C_{2v} symmetry with the Cr atom connecting with two P atoms

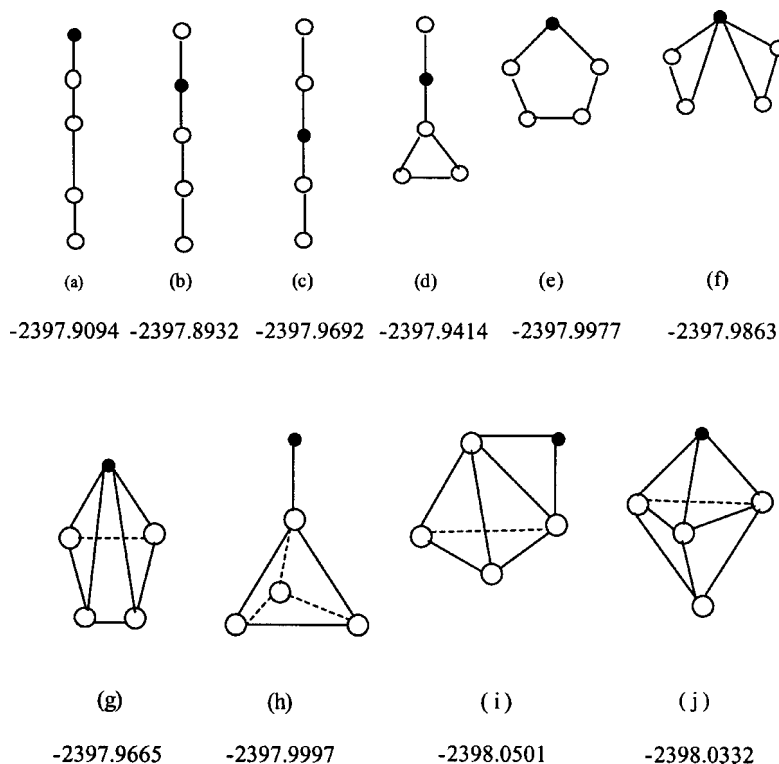


Figure 5. The proposed structures of $[\text{CrP}_4]^+$ evaluated by DFT calculation. (Note: the black circle stands for Cr atom while the white for P atom; the value below each model is the energy (Hartree) from calculation.)

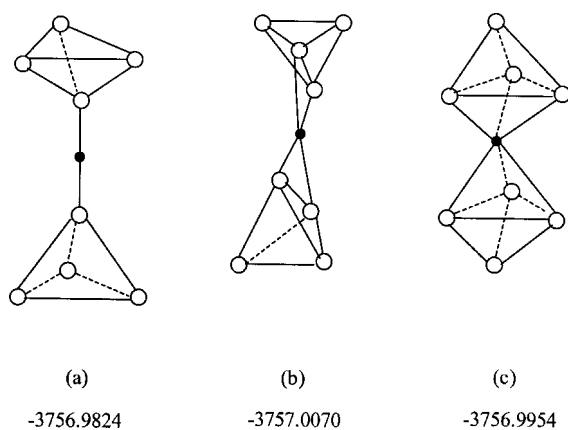


Figure 6. The proposed structures of $[\text{CrP}_8]^+$ evaluated by DFT calculation.

of the P_4 tetrahedron. The second most stable of this level of theory is structure (j), in which there are bonds between the Cr atom and three P atoms of the P_4 tetrahedron. Among the linear and planar structures, the more stable structures are (e) and (c) in which the four P atoms are symmetrically located, with P-P distances varying between 1.90–1.96 Å, indicating that the P-P bond may be a double bond (compare with the bond lengths 2.219 and 1.895 Å¹⁷ corresponding to the single and triple P-P bonds).

For $[\text{CrP}_8]^+$ we propose three structure models with the Cr atom located between the two P_4 tetrahedra (shown in Fig. 6). The most stable of these structures is (b), in which the Cr atom is connected to two P atoms of each tetrahedron. The structure (c), in which the Cr atom is connected to three P atoms of each tetrahedron, is more stable than (a) in which only one P atom of each tetrahedron is connected to the Cr atom.

For $[\text{Cr}_2\text{P}_2]^+$, four model structures are proposed (shown in Fig. 7). The most stable structure is (c), in which the four atoms form a stereo (i.e. 'non-planar') ring in which the two P atoms act as bridges between the two Cr atoms and there is also weak interaction between the two Cr atoms. Structure (d) is a planar ring in which Cr atoms and P atoms connect alternately and there is no bonding between the two Cr atoms or the two P atoms; this structure is more stable than the linear structures (a) and (b).

CONCLUSIONS

The Cr/P binary cluster ions were obtained by direct laser ablation on a solid sample and the UV laser photodissociation of some Cr/P cluster cations was studied. It was found that Cr/P cluster ions rich in phosphorus are easily produced, and the photodissociation of Cr/P cluster cations mainly proceeds via the following steps: P_2 and P_4 are lost first, and then Cr is expelled. The quantum-chemical (DFT) calculations suggest that P_4 tetrahedral structures are

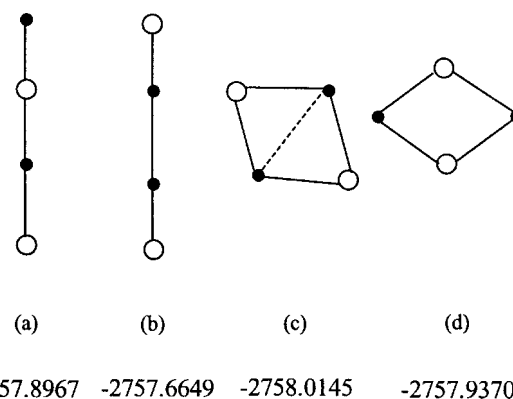


Figure 7. The proposed structures of $[\text{Cr}_2\text{P}_2]^+$ evaluated by DFT calculation.

preferentially formed for the clusters containing large numbers of P atoms. Where fewer than 4 P-atoms are present, the ring structures with bridging P atoms are more stable at this level of theory.

Acknowledgement

This work was supported by the National Science Foundation of China.

REFERENCES

- McElvany SW, Cassady CJ. *J. Phys. Chem.* 1990; **94**: 2057.
- Chevel R, Hirrien M, Sergent M. *Polyhedron.* 1986; **5**: 87.
- Mitchell PCH. *Wear* 1984; **100**: 281.
- Chianell RR. *Catal. Rev.-Sci. Eng.* 1984; **26**: 361.
- Cartier SF, May BD, Toleno BJ et al. *Chem. Phys. Lett.* 1994; **220**: 23.
- Guo BC, Kerns KP, Castleman AW. *Science* 1992; **255**: 1411.
- Armentrout PB, Loh SK, Ervin KM. *J. Am. Chem. Soc.* 1984; **106**: 116.
- Yu W, Freas RB. *J. Am. Chem. Soc.* 1990; **112**: 7126.
- Shi Y, Zhang N, Gao Z, Kong FA, Zhu QH. *J. Chem. Phys.* 1994; **101**: 9528.
- Yu ZD, Zhang N, Wu XJ, Gao Z, Zhu QH, Kong FA. *J. Chem. Phys.* 1993; **99**: 1765.
- Zhang N, Yu ZD, Wu XJ, Gao Z, Zhu QH, Kong FA. *J. Chem. Soc. Faraday Trans.* 1993; **89**: 1779.
- Shi Y, Yu ZD, Zhang N, Gao Z, Kong FA, Zhu QH. *J. Chin. Chem. Soc.* 1995; **42**: 455.
- Chen YQ, Xing XP, Liu P, Zeng R, Gao Z, Zhu QH. *Chem. J. Chinese Universities.* 2000; in press.
- Chen YQ, Xing XP, Liu P, Zeng R, Gao Z, Zhu QH. *Chin. J. Chem. Phys.* 2000; in press.
- Greenwood PF, Dance IG, Fisher KJ, Willett GD. *Inorg. Chem.* 1998; **37**: 6288.
- Wells AF. *Structural Inorganic Chemistry*, Oxford University Press: London 1975; 673.
- Xiang SF, Yan XS, Cao TL, Guo BN. *Inorganic Chemistry (Chin.)* 1975; **4**: 198.
- Gao Z, Kong FA, Wu XJ, Zhang N, Zhu QH et al. *Chin. J. Chem. Phys.* 1992; **5**: 343.
- Ma CS, Li HY, Zhang XG. *J. Chin. Phys. Chem.* 1996; **12**: 185.